

Article

Not peer-reviewed version

---

# *K2* Photometry and Long-Term H $\alpha$ Variability in Four Previously Unreported Be Stars

---

[Alan Pereira](#)<sup>†</sup>, Eduardo Janot-Pacheco<sup>†</sup>, [Jéssica M. Eidam](#)<sup>†</sup>, [Bergerson Van Hallen Vieira da Silva](#)<sup>‡,†</sup>, M. Cristina Rabello-Soares<sup>†</sup>, [Laerte Andrade](#)<sup>†</sup>, [Marcelo Emilio](#)<sup>‡,†</sup>

Posted Date: 3 March 2026

doi: 10.20944/preprints202603.0104.v1

Keywords: be stars; stellar variability; circumstellar disks



Preprints.org is a free multidisciplinary platform providing preprint service that is dedicated to making early versions of research outputs permanently available and citable. Preprints posted at Preprints.org appear in Web of Science, Crossref, Google Scholar, Scilit, Europe PMC.

Copyright: This open access article is published under a [Creative Commons CC BY 4.0 license](#), which permit the free download, distribution, and reuse, provided that the author and preprint are cited in any reuse.

Disclaimer/Publisher's Note: The statements, opinions, and data contained in all publications are solely those of the individual author(s) and contributor(s) and not of MDPI and/or the editor(s). MDPI and/or the editor(s) disclaim responsibility for any injury to people or property resulting from any ideas, methods, instructions, or products referred to in the content.

Article

# K2 Photometry and Long-Term H $\alpha$ Variability in Four Previously Unreported Be Stars

Alan Pereira <sup>1,†</sup> , Eduardo Janot-Pacheco <sup>4,†</sup> , Jéssica M. Eidam <sup>2,†</sup> ,  
Bergerson Van Hallen Vieira da Silva <sup>1,†,‡</sup> , M. Cristina Rabello-Soares <sup>3,†</sup> , Laerte Andrade <sup>5,†</sup>   
and Marcelo Emilio <sup>1,2,†\*</sup> 

<sup>1</sup> Universidade Estadual de Ponta Grossa, 84030-900 Ponta Grossa, PR, Brazil

<sup>2</sup> Observatório Nacional, MCTI, 20921-400 Rio de Janeiro, RJ, Brazil

<sup>3</sup> W. W. Hansen Experimental Physics Laboratory, Stanford University, Stanford, CA, 94305, USA

<sup>4</sup> Instituto de Astronomia, Geofísica e Ciências Atmosféricas, Universidade de São Paulo, 05509-090 São Paulo, SP, Brazil

<sup>5</sup> Laboratório Nacional de Astrofísica, Rua Estados Unidos 154, 37504-364 Itajubá, MG, Brazil

\* Correspondence: memilio@uepg.br

† These authors contributed equally to this work.

‡ Current address: Universidade Estadual de Maringá, 87020-900 Maringá, PR, Brazil

## Abstract

Classical Be stars are key laboratories for investigating how rapid rotation, pulsations, and mass loss couple to the formation and evolution of circumstellar decretion disks. However, few studies have combined *Kepler*/*K2* photometry with multi-epoch H $\alpha$  monitoring. Here we present four previously unclassified Be-type variable stars observed by *K2* (three in Campaign 11 and one in Campaign 15) and followed up with ground-based spectroscopy. We analyzed public PDC light curves and extracted variability frequencies using Lomb–Scargle periodograms and iterative prewhitening with a conservative detection threshold of  $S/N \geq 5$ . Optical spectra obtained at the Observatório Pico dos Dias (Brazil) over a multi-year baseline (2017–2025) include repeated H $\alpha$  observations and blue-region spectra for photospheric characterization. All targets show detectable *K2* variability on timescales from hours to days, with frequency spectra ranging from close multi-periodic components producing beating patterns to power dominated by low frequencies. Each star exhibits H $\alpha$  emission at multiple epochs, with long-term changes in line-profile morphology and equivalent width, indicating disk variability on year-long timescales. These results demonstrate that disk evolution can occur without conspicuous photometric outbursts over the time span of space-based observations, highlighting the diagnostic value of combining high-precision space photometry with long-term spectroscopy to characterize multiscale variability in Galactic Be stars.

**Keywords:** be stars; stellar variability; circumstellar disks

## 1. Introduction

Classical Be stars constitute a prominent laboratory for studying the interplay between rapid stellar rotation, pulsational phenomena, and the formation of circumstellar disks in hot stars. They are defined as non-supergiant B-type stars that show, or have shown at some stage of their evolution, Balmer line emission arising from a gaseous circumstellar environment. A comprehensive overview of their observational properties and physical interpretation is provided in the review of [1], which established the current consensus that classical Be stars host viscous, dust-free, quasi-Keplerian decretion disks fed by episodic or continuous mass loss from the central star.

Rapid rotation is widely recognized as a necessary ingredient of the Be phenomenon, with typical rotation rates approaching a substantial fraction of the critical velocity. However, rotation alone cannot account for the observed variability and recurrent disk-feeding events. Several physical mechanisms have therefore been proposed to explain how mass and angular momentum are transferred

from the stellar surface into orbit. Among these, non-radial pulsations (NRPs) have gained strong observational support, as multi-periodic pulsation patterns are commonly detected in Be stars and are often temporally associated with outbursts and disk variability [1]. Alternative or complementary scenarios, including magnetic activity or binary interaction, have also been discussed. However, large-scale organized magnetic fields appear to be rare among classical Be stars, and binarity alone cannot account for the phenomenon as a whole.

Photometric variability is one of the most conspicuous manifestations of the Be phenomenon and spans a large range of timescales and amplitudes, reflecting the complex interplay between stellar pulsations, rapid rotation, and circumstellar disk activity. While ground-based observations had long revealed complex and often irregular light curves in Be stars, space-based photometry has fundamentally transformed this field by providing uninterrupted, high-precision time series over extended periods.

Observations from missions such as *CoRoT* [2], *Kepler* [3], and more recently *TESS* [4] have shown that many Be stars exhibit rich frequency spectra characterized by groups of closely spaced peaks, amplitude modulation, and frequency beating. These pulsational signatures probe the stellar interior and thus serve as key diagnostics of the physical processes at work in rapidly rotating massive stars. In addition to coherent multi-periodic variability, Be stars frequently display transient photometric events (outbursts) marked by sudden brightness changes associated with enhanced mass loss and the feeding or restructuring of the circumstellar disk [5,6].

This coexistence of persistent pulsational signals with stochastic or quasi-cyclic variability highlights the need for long, continuous photometric monitoring. Such datasets enable not only the identification of dominant frequencies but also the investigation of their temporal stability and possible connections to disk formation, evolution, and dissipation processes. As a result, space-based photometry plays a central role in disentangling stellar and circumstellar contributions to the observed variability in Be stars.

In the specific context of *Kepler/K2* observations, recent systematic analyses have demonstrated that variability among B-type stars forms a continuum shaped primarily by stellar mass, rotation, and internal mixing, rather than by sharply separated instability classes. A detailed spectroscopic and seismic characterization of 122 B-type stars observed during *K2* Campaign 11 was presented by [7], while an extended variability classification of 73 B-type stars observed in Campaigns 13–18 was carried out by [8]. Together, these studies provided a homogeneous classification of nearly 200 B-type stars based on high-precision space photometry combined with ground-based spectroscopy. In both works, stars exhibiting classical Be characteristics were deliberately identified and excluded from the statistical samples owing to the additional complexity introduced by circumstellar disk variability and emission-line phenomena.

Following the failure of its second reaction wheel, the *Kepler* mission was reconfigured into the *K2* mission, operating as a sequence of observing campaigns along the ecliptic plane. Although originally designed for exoplanet detection, *K2* retained the key strengths of the original mission, including high photometric precision and the ability to obtain long, nearly continuous time series spanning several tens of days per campaign. For massive stars, including Be stars, this observational strategy provides a unique opportunity to investigate variability on short-to-intermediate timescales, from hours to months, enabling the detection of low-amplitude pulsation modes, amplitude modulation, and transient events that are difficult or impossible to characterize from the ground. Despite the reduced pointing stability relative to the original *Kepler* mission phase, advances in data-reduction pipelines have rendered *K2* light curves well suited for detailed frequency and time–frequency analyses.

Crucially, *K2*'s campaign-based observing strategy facilitates coordinated ground-based follow-up. When combined with spectroscopy, *K2* photometric data allow a direct comparison between stellar brightness variations and contemporaneous changes in spectroscopic diagnostics, such as emission-line variability tracing circumstellar disks. This synergy makes *K2* particularly valuable for studies aimed at disentangling stellar and circumstellar contributions to the observed variability in Be stars.

Despite the major advances brought by space-based photometry, which have firmly established the ubiquity and complexity of variability in Be stars, coordinated photometric and spectroscopic studies of individual Be stars with long temporal baselines remain comparatively limited. In particular, simultaneous or closely coordinated analyses of high-precision light curves and H $\alpha$  variability remain scarce, limiting our ability to directly associate photometric signatures with disk-related phenomena and mass-loss processes. This observational gap is further emphasized by the systematic exclusion of Be stars from large-scale *K2* variability classifications, owing to the additional complexity introduced by circumstellar emission and disk variability.

In this study, we fill this gap by reporting the discovery and analysis of four previously unclassified Be-type variable stars observed by the *Kepler/K2* mission, which have not previously been identified in the literature as Be-type variables (i.e., exhibiting both Be-type H $\alpha$  emission and associated photometric variability), followed by multi-epoch H $\alpha$  spectroscopy at the Observatório Pico dos Dias, Brazil. The primary objectives are: (i) to delineate their short-term photometric variability, (ii) to investigate long-term circumstellar disk evolution via H $\alpha$  diagnostics, and (iii) to examine the correlation between stellar pulsational behavior and disk-associated variability. This coordinated approach makes it possible to directly compare structural changes occurring over years with variability changes occurring on timescales of hours to days.

Because Be stars are frequently excluded from large-scale variability classifications owing to their circumstellar complexity, detailed case studies that combine space photometry with long-term disk monitoring remain comparatively scarce. This study, therefore, fills an important observational gap by providing robust frequency catalogs, multi-year H $\alpha$  equivalent-width time series, a systematic characterization of amplitude modulation and low-frequency variability consistent with stochastic processes, and reproducible analysis procedures that can serve as a reference framework for future investigations of pulsation–disk coupling in classical Be stars.

## 2. Materials and Methods

### 2.1. *Kepler/K2* Photometric Observations

The photometric data analyzed in this work were obtained by the *Kepler* space telescope during its *K2* mission, which provides high-precision space-based photometry using a single broad-bandpass filter spanning approximately 420–900 nm. This spectral response overlaps with the classical Johnson B, V, R, and I bands, making the data well-suited for variability studies of hot stars.

Among the four Be-type stars analyzed in this study, three were observed during *K2* Campaign 11 and one during Campaign 15. Campaign 11 was conducted between September and December 2016 and provided nearly continuous photometric monitoring for approximately 71 days. These observations were obtained under the Guest Observer program GO11127 (PI: M. Emilio), which targeted 122 candidate B-type stars with spectral types ranging from O9 to A0 selected from the SIMBAD database. The observations were acquired predominantly in long-cadence mode, with an effective integration time of approximately 30 minutes per exposure, and the Be stars analyzed here are part of the 32,884 long-cadence targets observed during this campaign. Owing to an error in the initial roll-angle configuration adopted to minimize solar torque on the spacecraft, Campaign 11 was divided into two observational segments.

The fourth Be-type star analyzed in this work was observed during *K2* Campaign 15, conducted between August and November 2017 under the Guest Observer program GO15099 (PI: M. Emilio). This campaign targeted a field toward the constellation of Scorpius and included 23,279 standard long-cadence targets, along with a smaller number of short-cadence observations. The field encompasses the outskirts of the Upper Scorpius association, one of the nearest OB associations, with an estimated age of approximately 11 Myr, making it particularly favorable for studies of variability in young and massive stars. As in Campaign 11, the observations used in this work were obtained predominantly in long-cadence mode.

In this study, we used publicly available *K2* light curves processed through the standard *Kepler* data reduction pipeline. The resulting Pre-search Data Conditioning (PDC) light curves were adopted for the photometric analysis presented here. All observation times are given in Barycentric Julian Date (BJD), accounting for the motion of the spacecraft relative to the Solar System barycenter. The light curves were then adjusted for systematic errors using the *K2* Systematics Correction (K2SC, version 2.0) software package Aigrain et al. [9], which minimizes the effect of spacecraft jitter on the data. This method uses a Gaussian process to correlate the star's two-dimensional CCD position with its photometric variability. The K2SC method provides performance comparable to the *K2* self-flatfielding method of Vanderburg and Johnson [10], but is better suited for studies of stellar variability.

We examined the default aperture masks for all targets to assess potential contamination from nearby sources. Significant contamination from two neighboring stars was identified only for HD 159571 (EPIC 240541552), located in a crowded field. A custom aperture mask was therefore generated using the `lightkurve` software package to minimize flux contamination. Figure A1 compares the original pipeline mask with the custom-defined aperture. For the remaining targets, the default masks were adopted.

### 2.2. Photometric Data Processing and Frequency Analysis

After describing the observational characteristics of the *K2* data, we now outline the procedures adopted for light-curve processing and frequency extraction. The PDC light curves used in this work were obtained from the public archive after processing by the standard *Kepler* Science Pipeline, which applies a sequence of calibration and correction steps at the pixel and light-curve levels to mitigate instrumental effects related to detector response, spacecraft pointing, and thermal variations.

For targets observed during *K2* Campaign 11, the segmentation caused by the change in spacecraft roll angle introduces a discontinuity in the raw time series. This effect is largely mitigated in the pipeline-processed PDC light curves used here. A visual inspection of all light curves was nevertheless performed to identify any remaining discontinuities or artifacts that could affect the frequency analysis.

The analysis of photometric variability was carried out using Fourier-based techniques. Frequency spectra were computed using the Lomb–Scargle periodogram [11], which is well suited to unevenly sampled time series and is commonly used in the analysis of space-based photometric data. To extract individual periodic components, we applied an iterative prewhitening procedure [12]. At each step, the frequency corresponding to the highest peak in the periodogram was identified and fitted together with previously detected frequencies using a non-linear least-squares approach. The fitted signal was then subtracted from the original light curve, and the procedure was repeated on the residuals.

The iterative process was stopped when the signal-to-noise ratio of the highest remaining peak dropped below a threshold of  $S/N = 5$ . This conservative criterion, previously adopted in *K2* asteroseismic studies [13], is also applied here to minimize the inclusion of spurious frequencies and ensure the robustness of the detected signals. Frequencies associated with unusually large formal uncertainties were also discarded. The resulting set of frequencies, therefore, represents a balance between sensitivity to low-amplitude variability and the reliability of the detections.

The effective frequency range accessible in our analysis is constrained by the time sampling and total duration of the observations. For long-cadence *K2* data, periods shorter than the Nyquist limit imposed by the 30 min sampling and periods comparable to or longer than the total campaign duration were not considered.

### 2.3. Spectroscopic Observations

Spectroscopic observations were conducted to characterize the atmospheric properties of the targets and to monitor variability in the  $H\alpha$  line as a tracer of circumstellar disk activity. The data were obtained between March 2017 and March 2025 at the Observatório Pico dos Dias (OPD), operated by the National Laboratory of Astrophysics (LNA) in Brazópolis, Minas Gerais, Brazil.

Observations were carried out with the 1.6 m Perkin–Elmer Ritchey–Chrétien telescope. Spectra obtained before 2020 were acquired with the Cassegrain spectrograph coupled to a CCD detector,

providing a typical spectral resolving power of  $R \sim 10^4$  and a signal-to-noise ratio of approximately 100 in the continuum. From 2020 onwards, additional spectra with higher resolving power, up to  $R \sim 25,000$ , were obtained using the Coudé spectrograph for selected targets.

Two main wavelength configurations were employed. The first covered the blue spectral region, approximately 3990–5110 Å, including diagnostic lines of hydrogen, neutral helium (He I), and magnesium (Mg II), which are commonly used for spectral classification and atmospheric parameter determination in B-type stars. The second configuration focused on the red spectral region, from about 6040 to 6950 Å, encompassing the H $\alpha$  line, and was specifically designed to investigate emission-line variability associated with the circumstellar disks of Be stars.

#### 2.4. Spectroscopic Data Reduction and H $\alpha$ Measurements

The spectroscopic data were reduced using standard procedures implemented in the IRAF (Image Reduction and Analysis Facility) software package [14]. The reduction steps included bias subtraction, flat-field correction, cosmic-ray removal, and one-dimensional spectral extraction. Wavelength calibration was performed using comparison lamp spectra acquired with the same instrumental configuration as the science observations, ensuring a consistent wavelength solution for each observing run.

After extraction and wavelength calibration, all spectra were normalized to the local continuum. Continuum normalization was achieved by fitting low-order polynomial functions to line-free regions adjacent to the spectral features of interest, with particular care taken in the vicinity of the H $\alpha$  line to avoid contamination from emission wings or nearby absorption features. This approach enables a consistent comparison of line profiles obtained at different epochs and with different instrumental setups.

The variability of the circumstellar disk was investigated by measuring the H $\alpha$  line profile. For each spectrum, the equivalent width (EW) of the H $\alpha$  line was measured from the normalized spectra using the EQUIVALENT\_WIDTH routine from the SPECUTILS package (part of the Astropy project; Astropy Collaboration et al. [15,16]). We adopted the convention that positive EW values indicate absorption and negative values indicate emission. To minimize contamination from adjacent spectral features, continuum reference regions on both sides of the H $\alpha$  line were manually defined for each spectrum. The resulting EW measurements provide a quantitative proxy for changes in the kinematic and structural properties of the emitting circumstellar material, and all measurements were performed consistently to ensure internal homogeneity across the dataset.

When multiple spectra were available for a given target, the temporal evolution of the H $\alpha$  EW was examined over the full spectroscopic monitoring interval, which in several cases extends well beyond the time span covered by the K2 photometric observations. This long-term spectroscopic information provides context for the state and evolution of the circumstellar disk and is used to qualitatively compare disk-related variability with the photometric behavior observed during the K2 campaigns, as discussed in the following sections.

### 3. Results

The sample analyzed in this work consists of four classical Be stars observed with the *Kepler* space telescope during its K2 mission and followed up with ground-based spectroscopy. Three targets were observed during K2 Campaign 11, and one during Campaign 15. All four stars exhibit clear signatures of variability in both photometric and spectroscopic data, making them well suited for combined observational analysis.

High-precision K2 photometry reveals detectable brightness variability in all targets over the duration of the campaigns, which span several tens of days. In parallel, optical spectroscopy obtained over a much longer time baseline, extending over several years for all targets, provides multiple H $\alpha$  observations for each star, revealing persistent emission and temporal variability associated with their circumstellar disks. The difference in temporal coverage between the two datasets allows the photometric variability to be examined on short to intermediate timescales, while the spectroscopic observations place these variations within a longer-term context of circumstellar disk evolution.

In the following subsections, the results for each star are presented individually using a consistent structure. For each object, we first describe the photometric variability detected in the *K2* light curves, followed by an analysis of the H $\alpha$  line behavior and its temporal evolution. Each subsection concludes with a summary linking the photometric and spectroscopic findings. Table 1 lists the significant frequencies identified through the pre-whitening procedure, together with their corresponding amplitudes, for all four stars.

**Table 1.** Extracted frequencies and amplitudes for the analyzed Be stars. The value in parentheses represents the uncertainty in the last visible digit(s) of the frequencies extracted via the prewhitening procedure, calculated according to Equation (2) of Degroote et al. [12].

HD 155291 EPIC 230653391		HD 159571 EPIC 240541552		HD 138872 EPIC 249150896		HD 315823 EPIC 240426061	
Freq [d <sup>-1</sup> ]	Amp [ppm]	Freq [d <sup>-1</sup> ]	Amp [ppm]	Freq [d <sup>-1</sup> ]	Amp [ppm]	Freq [d <sup>-1</sup> ]	Amp [ppm]
0.035(1)	41	0.0211(8)	85	0.024(1)	12	0.0391(6)	154
0.062(1)	42	0.0377(6)	155	0.0367(6)	39	0.057(1)	68
0.110(1)	34	0.0594(7)	130	0.0549(6)	31	1.010(1)	56
1.662(1)	52	0.136(1)	38	0.065(1)	10	1.0224(8)	101
1.710(1)	46	0.2621(7)	171	0.0842(8)	21	1.095(2)	42
1.7286(5)	159	0.274(1)	53	0.110(1)	14		
3.392(2)	35	0.5299(9)	70	0.1237(7)	26		
3.420(1)	44	2.469(1)	53	0.1565(9)	15		
3.4490(7)	99	2.482(2)	36	0.171(1)	12		
3.4704(9)	68	2.4959(9)	124	0.1835(8)	20		
3.701(2)	27	2.514(1)	66	0.220(1)	13		
6.899(2)	28	2.974(1)	46	0.244(1)	11		
		2.991(1)	86	0.269(1)	11		
		3.019(1)	74	0.290(1)	10		
		3.033(1)	42	0.491(1)	11		
		3.0442(9)	121	0.519(1)	13		
		3.278(1)	69	0.7080(3)	82		
		3.343(2)	32	0.7207(6)	30		
		5.098(2)	28	1.406(1)	11		
		6.262(2)	27	1.4228(4)	62		
		19.442(4)	14	1.4344(7)	26		
				1.473(1)	10		
				1.5394(8)	19		
				1.551(1)	14		
				1.5674(9)	16		
				1.615(1)	10		
				2.137(1)	11		
				2.150(1)	11		

### 3.1. HD 155291

HD 155291 (EPIC 230653391, TIC 101669617) has been classified as a B9IV star with a visual magnitude of  $V = 7.4$  mag [17]. The star was observed by the *Kepler* space telescope during *K2* Campaign 11, in a field projected toward the constellation Ophiuchus. To our knowledge, no previous study has combined space-based photometry with long-term spectroscopic monitoring for this object.

The *K2* light curve of HD 155291 exhibits clear variability over the duration of Campaign 11. The Fourier analysis reveals multiple significant frequencies, indicative of a multi-periodic signal rather than simple rotational modulation. The detected variability is characterized by low-amplitude brightness fluctuations with stable periodic components throughout the campaign, as illustrated in the

light curve and corresponding frequency spectrum (Figure 1). No large-amplitude transient events are observed in the photometric data during the K2 time span.

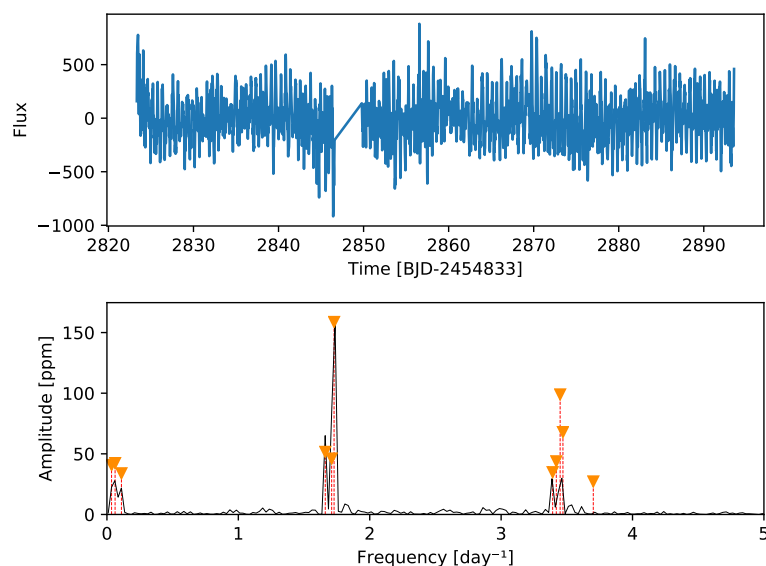


**Figure 1.** K2 photometric light curve and corresponding Lomb–Scargle frequency spectrum of HD 155291, observed during Campaign 11. The upper panel shows the detrended PDC light curve over time, while the lower panel displays the amplitude spectrum derived from the Fourier analysis. Prominent peaks indicate periodic variability detected during the campaign.

Multi-epoch spectroscopic observations of HD 155291 obtained over a multi-year baseline reveal persistent H $\alpha$  emission, confirming its Be-star nature. The first H $\alpha$  spectrum of this star was obtained in March 2018, when a strong emission profile was observed, and subsequent observations were carried out at eight distinct epochs extending through March 2025. Over this interval, the H $\alpha$  line profile exhibits measurable variability in both width and shape. The temporal evolution of the H $\alpha$  equivalent width (EW) indicates systematic variations on timescales much longer than those sampled by the K2 photometry, providing evidence for long-term changes in the circumstellar environment rather than a static emission configuration (Figure 2).

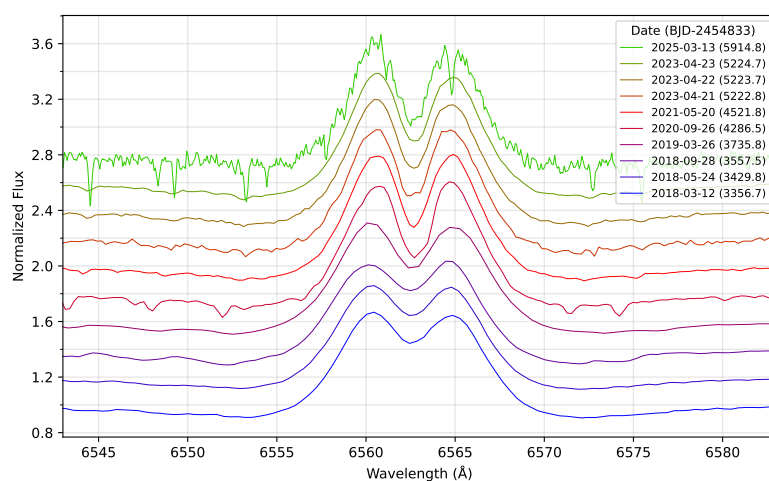


**Figure 2.** Multi-epoch H $\alpha$  line profiles of HD 155291 obtained between March 2018 and March 2025. The spectra are presented as normalized flux versus wavelength, with each observation date represented by a distinct color, as indicated in the figure annotations. For clarity, individual profiles are vertically offset to avoid overlap. The sequence reveals clear changes in the shape and width of the H $\alpha$  emission line over the years, indicating temporal variability in the circumstellar disk.

HD 155291 displays photometric variability on timescales of hours, as revealed by *K2* observations, together with long-term spectroscopic variability of the  $H\alpha$  line monitored over several years. The frequency spectrum of the *K2* light curve is dominated by two closely spaced frequencies around 1.7 cycles per day, corresponding to characteristic periods of approximately 14 hours. The proximity of these frequencies produces a clear beating pattern in the time-domain light curve, characterized by periodic modulation of the variability amplitude. In addition to the fundamental frequencies, significant power is detected at the first harmonic, consistent with coherent pulsational variability.

While the frequency content of the photometric signal remains stable throughout the *K2* campaign, the light curve exhibits pronounced amplitude modulation due to beating between the close frequencies. In contrast, the  $H\alpha$  measurements reveal substantial variations in the equivalent width (EW) (Figure 2) of the emission line over the seven-year spectroscopic baseline, indicating long-term changes in the circumstellar disk. Taken together, the photometric and spectroscopic observations establish HD 155291 as a Be star exhibiting variability on multiple temporal scales, providing a well-defined observational case for exploring the relationship between short-term stellar variability and longer-term disk evolution.

Additional information on the stellar photospheric properties of HD 155291 is provided by blue-region spectroscopy obtained at different epochs. Figure 4 shows representative normalized spectra covering key diagnostic lines of hydrogen and helium commonly used for spectral classification and atmospheric analysis in B-type stars. These data allow a qualitative assessment of the photospheric line profiles. Classical stellar classification criteria based on the appearance of the Balmer line wings and He I, OII, Si III and Mg II line ratios [18–20] were applied to the blue spectrum of Figure 4. Our classification indicates a B8III stellar type.

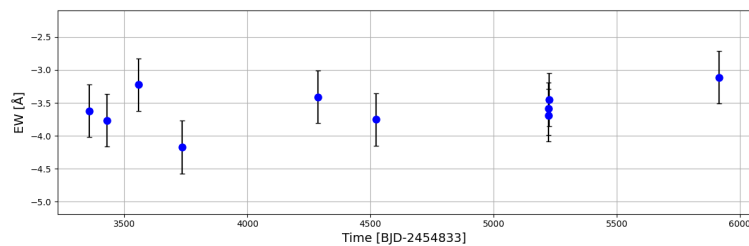


**Figure 3.** Temporal evolution of the  $H\alpha$  equivalent width (EW) of HD 155291 derived from the multi-epoch spectra shown in Figure 2. The EW measurements trace the long-term variability of the  $H\alpha$  emission over several years, reflecting changes in the circumstellar disk. Note that EW values follow the convention where positive values indicate absorption and negative values indicate emission. Error bars represent the  $1\sigma$  uncertainties of the EW measurements, conservatively estimated from spectral quality. To avoid underestimating the uncertainties, the adopted error bars were set larger than the typical EW dispersion measured in non-emission B-type stars observed with the same instrumental configuration.

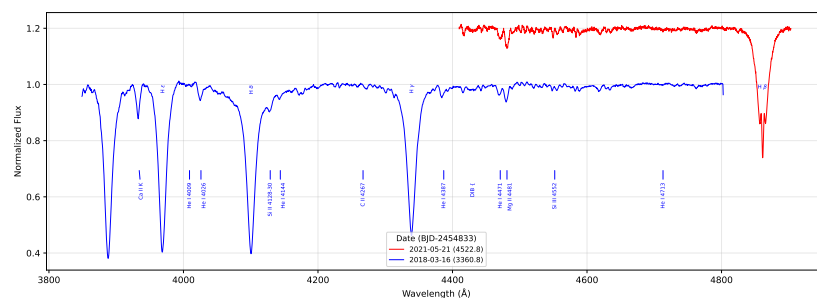


**Figure 4.** Normalized blue-region spectra of HD 155291 obtained at two different epochs. The upper spectrum covers the wavelength range from 3850 to 4800 Å and was acquired in March 2016, showing prominent absorption features including the Balmer lines  $H\epsilon$ ,  $H\delta$ , and  $H\gamma$ , as well as He I  $\lambda 4026$ , He I  $\lambda 4387$ , He I  $\lambda 4471$ , and Mg II  $\lambda 4481$ . The lower spectrum, obtained in May 2021, spans 4410–4900 Å and includes the  $H\beta$  line. Both spectra are continuum-normalized and vertically offset in flux for clarity.

### 3.2. HD 159571

HD 159571 (EPIC 240541552, TIC 199983403) is classified as a B8V star [17] with apparent visual magnitude  $V = 9.0$  mag. The *Kepler* space telescope observed the star during *K2* Campaign 11.

High-precision *K2* photometry reveals clear brightness variability in HD 159571 on timescales of hours to a few days. The *K2* light curve and corresponding Lomb–Scargle frequency spectrum are shown in Figure 5. The frequency spectrum is dominated by low-frequency power, with additional significant peaks around  $2.5$  and  $3 \text{ day}^{-1}$  which are characteristic of non-radial pulsations commonly observed in classical Be stars and naturally explain the beating pattern visible in the light curve.

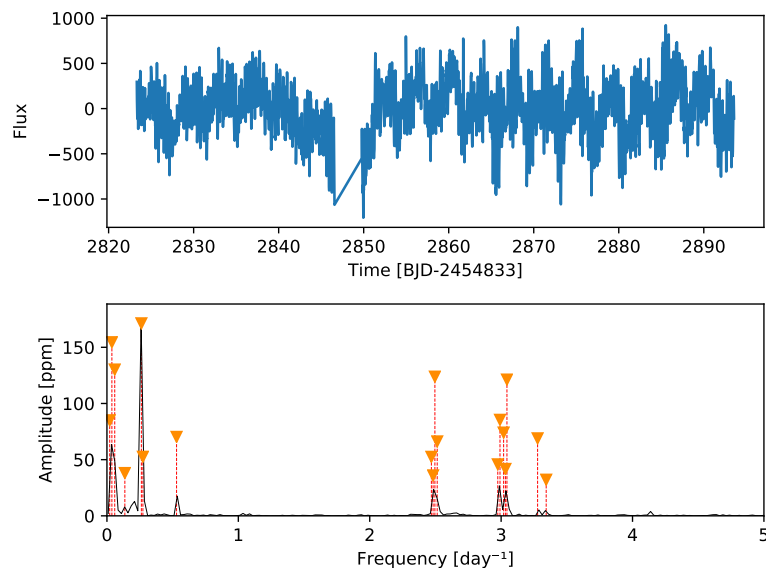


**Figure 5.** *K2* light curve (upper panel) and Lomb–Scargle frequency spectrum (lower panel) of HD 159571 observed during Campaign 11. Low-frequency components dominate the frequency spectrum, while additional significant peaks are detected around  $3 \text{ day}^{-1}$ , consistent with pulsational variability commonly observed in Be stars. The low-frequency signals may be associated with SLF-type variability, rotational modulation, long-term trends, and residual instrumental effects (see text).

The presence of strong low-frequency components in the star’s power spectrum could be due to a relatively new type of variability, stochastic low-frequency variability (SLF). This phenomenon was first detected in a few O stars by the CoRoT satellite and later observed systematically in hundreds of massive stars in *K2* and *TESS* data (e.g., [21–23]). SLF-type variability was observed by Pereira et al. [7] in almost half of a sample of SPB stars observed during *Kepler/K2* campaign 11. Alternatively, the low-frequency components could reflect a combination of residual instrumental systematics and long-term trends that the pipeline correction did not fully remove.

Multi-epoch spectroscopic observations of HD 159571 obtained over several years reveal persistent  $H\alpha$  emission, confirming its Be-star nature. The  $H\alpha$  line was first observed in emission in May 2018 and subsequently monitored at six epochs until April 2023. The normalized  $H\alpha$  profiles are presented in Figure 6, where clear variations in line shape and width are evident across the observing period.

The temporal evolution of the  $H\alpha$  equivalent width, shown in Figure 7, indicates variability on timescales of years. A sinusoidal function with a period of approximately 2550 days can be fitted to the current dataset ( $R_{adj}^2 = 0.92$ ), but this should be regarded primarily as a descriptive representation rather than evidence for a stable periodic cycle, particularly given the limited temporal coverage and the relatively small number of spectroscopic epochs. Long-term quasi-cyclic variations in  $H\alpha$  emission have been reported in several Be stars, including Pleione [24,25], although such behavior may arise from different mechanisms, including intrinsic disk evolution. At present, there is insufficient evidence to attribute the observed modulation to binarity or any specific external influence, and continued spectroscopic monitoring will be necessary to determine whether the observed pattern reflects a stable

physical cycle or a transient manifestation of the complex, potentially stochastic variability inherent to Be-star disks.

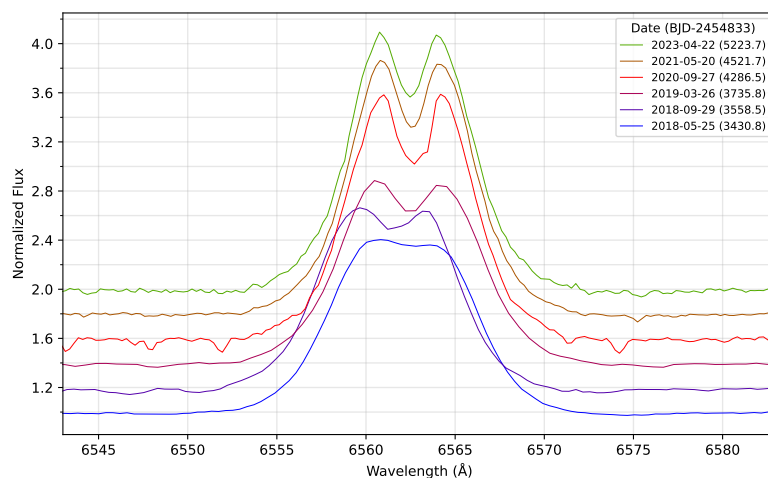


**Figure 6.** Normalized H $\alpha$  line profiles of HD 159571 obtained at six different epochs between May 2018 and April 2023, presented in the same format as Figure 2.

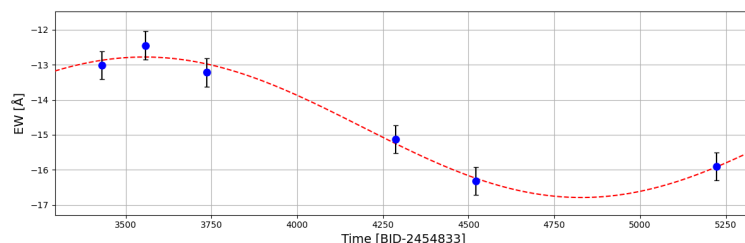


**Figure 7.** Temporal evolution of the H $\alpha$  equivalent width (EW) of HD 159571 measured from the spectra shown in Figure 6. The EW values exhibit significant variations over the multi-year monitoring interval, reflecting long-term changes in the circumstellar disk properties. The red dashed line represents a sinusoidal fit with a period of 2550 days, suggesting a quasi-periodic modulation in the disk's emission.

A representative blue-region spectrum of HD 159571 obtained in 2018 is shown in Figure 8. Applying the classical classification criteria described above results in a B8V spectral type, consistent with the literature classification [17].

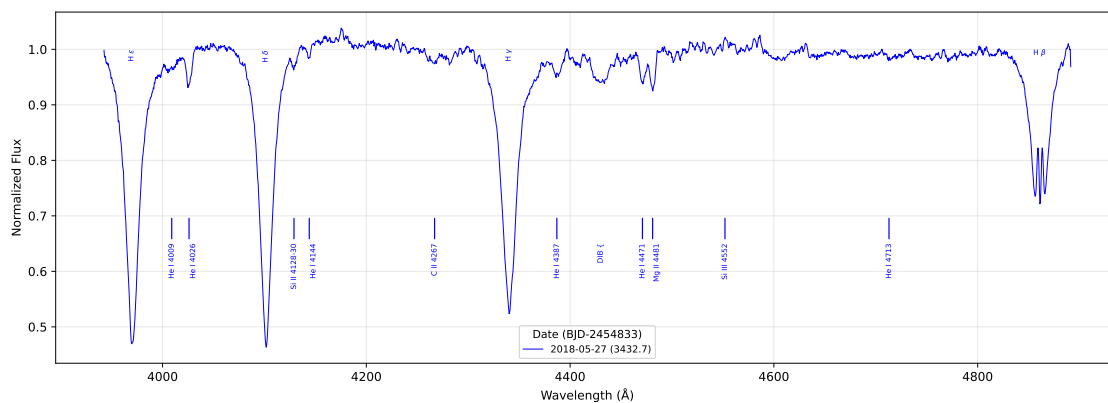


**Figure 8.** Normalized blue-region spectrum of HD 159571 obtained in 2018, covering the wavelength range from approximately 3900 to 4900 Å. The spectrum includes prominent diagnostic lines of the Balmer series (H $\epsilon$ , H $\delta$ , H $\gamma$ ), neutral helium (He I  $\lambda$ 4026,  $\lambda$ 4387,  $\lambda$ 4471), and magnesium (Mg II  $\lambda$ 4481), commonly used for spectral classification and atmospheric characterization of B-type stars.

HD 159571 exhibits variability on multiple temporal scales, combining short-timescale photometric variability dominated by pulsational frequencies with long-term spectroscopic variability associated

with changes in its circumstellar disk. The *K2* photometry probes stellar variability on timescales of hours to days, while the multi-year  $H\alpha$  monitoring traces the slower evolution of the disk structure and kinematics. Together, these observations establish HD 159571 as a representative Be star in which stellar pulsations and circumstellar disk variability coexist, offering a valuable case for investigating the connection between short-term stellar variability and long-term disk evolution.

### 3.3. HD 138872

HD 138872 (EPIC 249150896, TIC 186902398) is classified as a B9 III star [26] with apparent visual magnitude  $V = 8.8$  mag. The star was observed by the *Kepler* space telescope during *K2* Campaign 15, in a field located toward the constellation of Libra.

The *K2* light curve of HD 138872 reveals photometric variability over the duration of Campaign 15, as shown in Figure 9. The star exhibits only a few significant frequencies, and a prominent peak dominates the Lomb–Scargle frequency spectrum at  $0.71$  cycles  $\text{day}^{-1}$ , corresponding to a characteristic timescale of about 1.4 days. This frequency corresponds to the strongest photometric signal detected during the campaign. It is consistent with the variability commonly observed in Be stars, potentially due to non-radial pulsations or rotational modulation. Additional low-frequency power is also present, indicating the possible presence of SLF variability (see above).

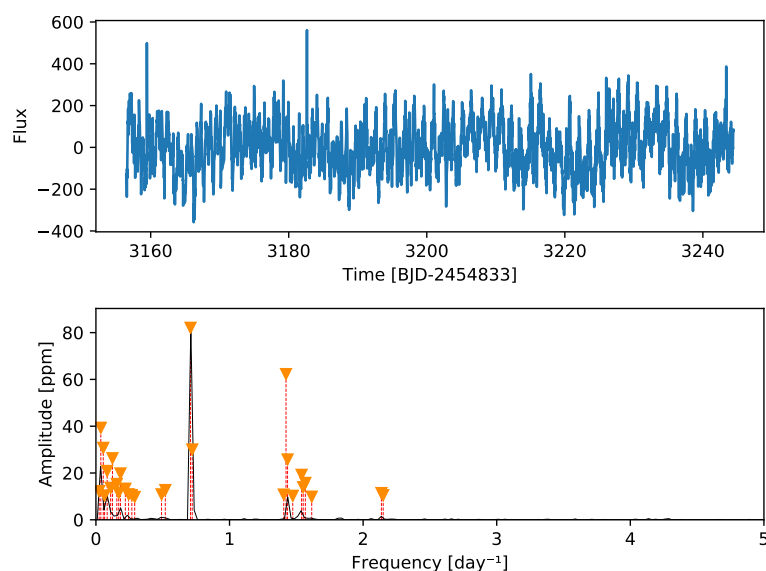


**Figure 9.** *K2* light curve (upper panel) and Lomb–Scargle frequency spectrum (lower panel) of HD 138872 observed during Campaign 15. The frequency spectrum is dominated by a prominent peak at  $0.71$  cycles  $\text{day}^{-1}$ , corresponding to the strongest photometric variability detected during the campaign. Note the numerous frequencies below about  $0.5$  cycles  $\text{day}^{-1}$  that are typical of SLF variations (see text).

Multi-epoch spectroscopic monitoring of HD 138872 reveals persistent  $H\alpha$  emission, confirming its Be-star nature. Figure 10 presents eleven normalized  $H\alpha$  line profiles obtained between March 2017 and April 2023. The line profiles exhibit clear variations in both shape and width across epochs, indicating changes in the kinematic and structural properties of the circumstellar disk over timescales of several years. Although the double-peaked emission peaks occasionally rise above the continuum at some epochs, the bulk of the area of this very broad line remains below the continuum, indicating that the absorption component dominates over the emission contribution.

The temporal evolution of the  $H\alpha$  equivalent width (EW), shown in Figure 11, further illustrates this long-term variability. The EW measurements exhibit significant fluctuations throughout the monitoring interval, reflecting variations in the density and extent of the emitting circumstellar material rather than a static disk configuration.

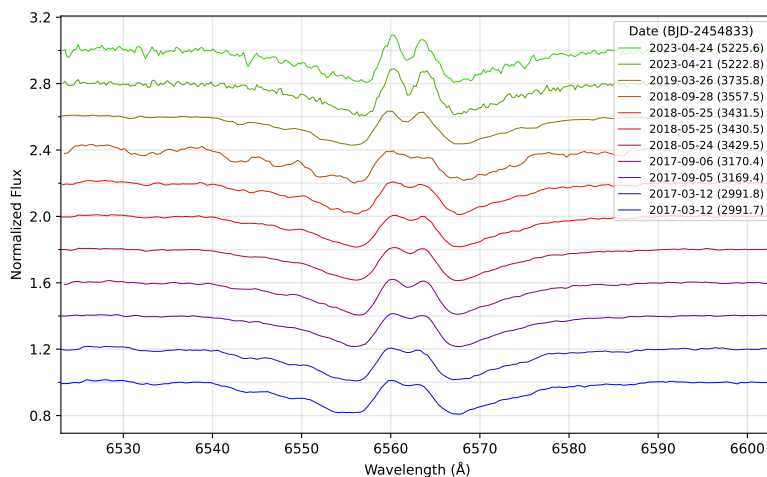


**Figure 10.** Normalized  $H\alpha$  line profiles of HD 138872 obtained at eleven different epochs between March 2017 and April 2023, presented in the same format as Figure 2.

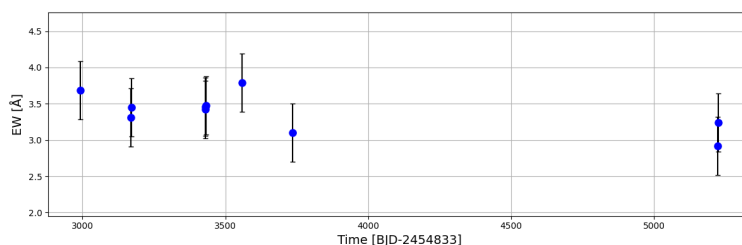


**Figure 11.** Temporal evolution of the  $H\alpha$  equivalent width (EW) of HD 138872 measured from the spectra shown in Figure 10. The EW values exhibit significant variability over the multi-year monitoring interval, indicating long-term changes in the physical conditions and structure of the circumstellar disk.

Figure 12 shows normalized blue-region spectra of HD 138872 obtained at multiple epochs between March 2017 and September 2022, covering the wavelength range from approximately 3900 to 4900 Å. Again, we applied the spectral classification criteria mentioned above to HD 138872 and concluded that it is a B8III star.

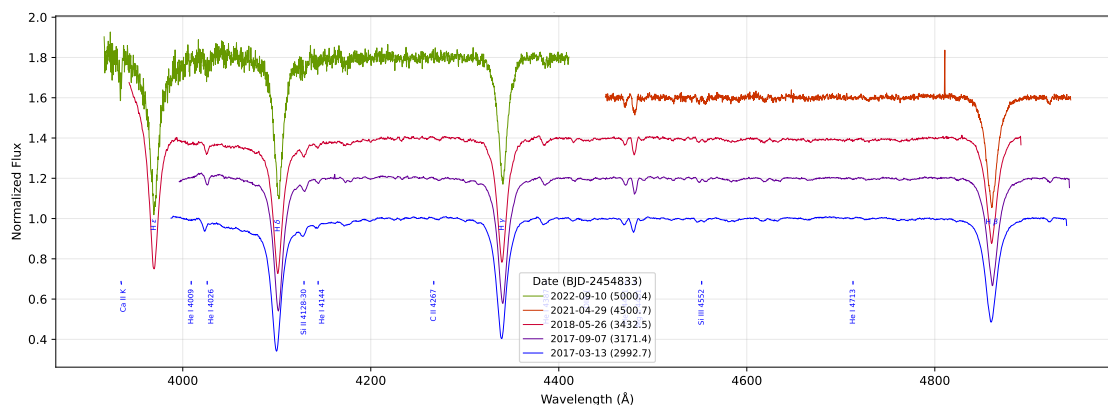


**Figure 12.** Normalized blue-region spectra of HD 138872 obtained between March 2017 and September 2022, covering the wavelength range 3900–4900 Å. Similar to Figure 2, spectra are color-coded by observation date and vertically offset for clarity. The main Balmer, He I, and Mg II diagnostic lines used for B-type stellar classification are visible.

HD 138872 exhibits detectable photometric variability on timescales of order one day, as revealed by high-precision *K2* observations, together with pronounced long-term spectroscopic variability of the  $H\alpha$  line over several years. The combination of SLF, short-timescale photometric variability and multi-year evolution of the emission-line profiles indicates an active and evolving circumstellar disk.

### 3.4. HD 315823

HD 315823 (EPIC 240426061, TIC 187134762) is classified as a B8-type star [27] with apparent visual magnitude  $V = 9.9$  mag. The star was observed by the *Kepler* space telescope during *K2* Campaign 11.

The *K2* light curve of HD 315823 exhibits clear photometric variability over the duration of Campaign 11, as shown in Figure 13. The Lomb-Scargle frequency spectrum shows just a few frequencies, dominated by low-frequency components with the highest amplitudes, indicating variability on timescales of several days that could be due to the SLF phenomenon (see above). Such low-frequency signals may also be related to rotational modulation. In addition, significant peaks are detected at frequencies around 1 cycle day<sup>-1</sup>, a characteristic timescale commonly observed in classical Be stars and often associated with non-radial pulsations.

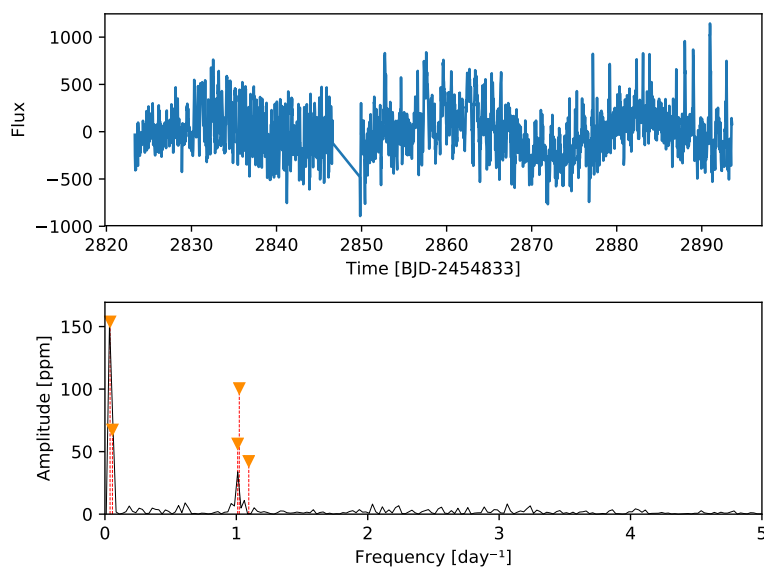


**Figure 13.** *K2* light curve (upper panel) and Lomb–Scargle frequency spectrum (lower panel) of HD 315823 observed during Campaign 11. The frequency spectrum is dominated by low-frequency components with the highest amplitudes, which may be associated with rotational modulation or SLF-type variability (see text). Additional significant peaks are detected at frequencies around 1 cycle day<sup>-1</sup>, consistent with pulsational variability commonly observed in Be stars.

Spectroscopic observations of HD 315823 reveal H $\alpha$  emission at two epochs, confirming the presence of a circumstellar disk. Figure 14 presents normalized H $\alpha$  line profiles obtained in May 2018 and May 2021. The comparison between the two spectra shows noticeable changes in the line profile, including variations in shape and width, indicating that the circumstellar disk is not static and undergoes structural or kinematic evolution on multi-year timescales.

The normalized blue-region spectrum of HD 315823 obtained in May 2018 is shown in Figure 15. The spectrum covers the wavelength range from approximately 3800 to 4800 Å and we applied the above-mentioned spectral classification criteria based on HeI line ratios and Balmer line profiles. We concluded that HD 315823 is a B8III-IV star.

HD 315823 thus displays photometric variability dominated by low-frequency signals on timescales of days, together with additional variability near 1 cycle day<sup>-1</sup> typical of Be stars. The detection of H $\alpha$  emission at multiple epochs and the observed changes in the line profile over several years indicate an evolving circumstellar disk.

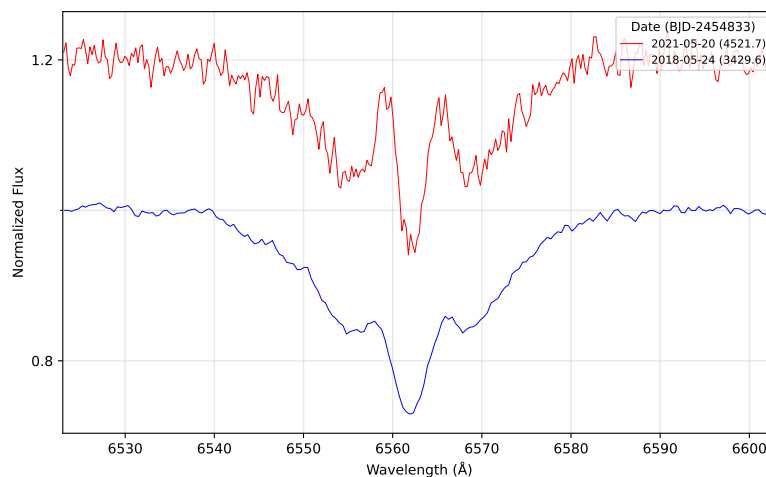


**Figure 14.** Normalized  $H\alpha$  line profiles of HD 315823 obtained in May 2018 and May 2021, presented in the same format as Figure 2.

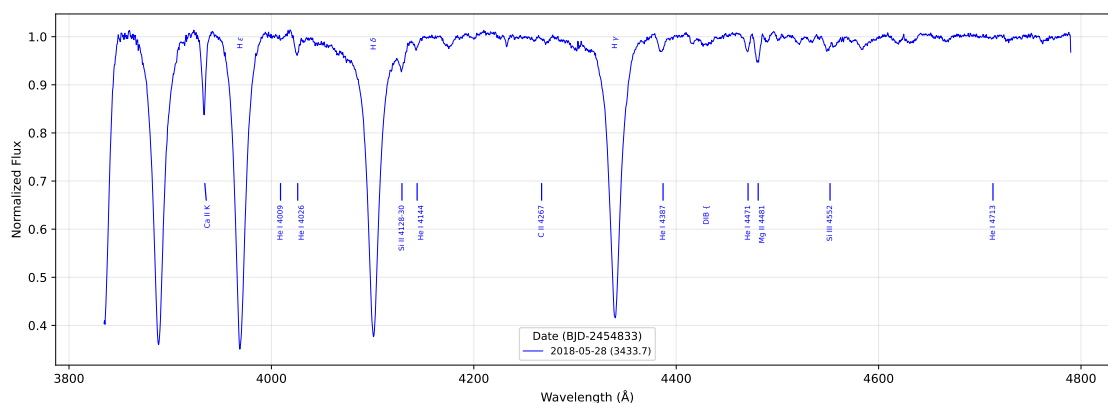


**Figure 15.** Normalized blue-region spectrum of HD 315823 obtained in May 2018, covering the wavelength range from approximately 3850 to 4800 Å. The spectrum displays prominent Balmer lines and neutral helium features commonly used for the spectral classification and atmospheric characterization of B-type stars.

#### 4. Discussion

Our results show that short-term pulsational variability can occur alongside the long-term evolution of circumstellar disks, including relatively bright Be stars that have received limited prior attention. This behaviour aligns with recent observational surveys indicating that variability and disk-related phenomena in Be stars are common and often episodic across a wide range of environments. Dedicated spectroscopic monitoring programs have demonstrated cycles of disk formation and dissipation, facilitating the identification of previously unknown Be stars through the detection of  $H\alpha$  emission (e.g., [28]). In parallel, space missions such as *Kepler*, *Kepler/K2*, and *TESS* have revealed a diverse range of variability patterns, including multi-periodic pulsations. Systematic searches (e.g., [29,30]), incorporating mid-infrared monitoring with *WISE* and extensive optical light-curve surveys of Be stars, also link photometric variability with changes in the circumstellar disk [31,32].

In this observational context, the four stars analyzed here should not be regarded as isolated cases, but rather as representative examples of Be stars whose variability becomes clearer when high-precision space photometry is combined with multi-epoch spectroscopic monitoring. *K2* photometry reveals short-timescale multi-periodic pulsations and, in some cases, significant low-frequency variability.  $H\alpha$  spectroscopy indicates ongoing structural evolution of the circumstellar disks. A main finding from this combined analysis is that disk changes can occur without conspicuous photometric outbursts over the time span of space-based observations, suggesting that such evolution may reflect cumulative or intermittent mass-loss processes. Despite the modest sample size, the observed variability patterns closely resemble those found in recent large surveys. These findings highlight the multiscale nature

of variability within individual Be stars and emphasize the importance of coordinated photometric observations and long-term spectroscopic monitoring for a comprehensive understanding of the Be phenomenon.

One limitation of the current study is that the *K2* campaigns were short, making it difficult to directly connect short-term pulsations to specific disk-feeding events. Future missions such as *PLATO* [33], owing to their substantially longer uninterrupted photometric baselines, will enable direct tests of whether the observed short-term pulsations and long-term disk variability persist over multi-year timescales. When combined with systematic spectroscopic monitoring, such datasets will provide stronger constraints on the physical coupling between stellar pulsations, rapid rotation, and circumstellar disk evolution.

**Author Contributions:** Conceptualization, methodology, validation, formal analysis, investigation, and writing, review and editing, all authors; software and data curation, B.S., A.P., and J.M.E.; resources, supervision, project administration, and funding acquisition, M.E., M.C.R.-S., and E.J.-P.; writing original draft preparation and visualization, all authors; observation of stellar spectra at OPD, B.S., A.P., L.A., M.E., and J.M.E. All authors have read and agreed to the published version of the manuscript.

**Funding:** This study was financed in part by the Coordenação de Aperfeiçoamento de Pessoal de Nível Superior—Brazil (CAPES)—Finance Code 001, by the Fundação de Amparo à Pesquisa do Estado de São Paulo (FAPESP) through grant 2016/13750-6. M.E. gratefully acknowledges the financial support of the “Fenômenos Extremos do Universo” project, Fundação Araucária, grant 348/2024.

**Data Availability Statement:** The *K2* data presented in this study are openly available in the Mikulski Archive for Space Telescopes (MAST), which can be found at <https://archive.stsci.edu/missions-and-data/k2> (accessed on 10 June 2025).

**Acknowledgments:** This paper includes data collected by the *K2* mission. Funding for the *K2* mission was provided by NASA’s Science Mission Directorate. This paper is also based on observations obtained at the Pico dos Dias Observatory/LNA/MCTI.

**Conflicts of Interest:** The authors declare no conflicts of interest.

## Appendix A. Custom Mask

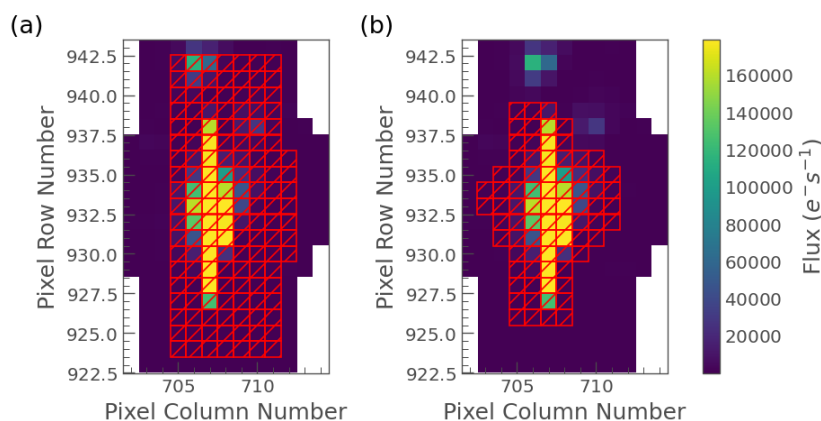


**Figure A1.** Aperture mask selection for HD 159571 (EPIC 240541552). (a) Default pipeline aperture mask (red hatched region), which includes pixels contaminated by flux from nearby sources. (b) Custom aperture mask defined in this work, designed to exclude contaminating pixels from adjacent objects while preserving the target flux.

## Appendix B. *TESS* Light Curve

We reviewed the available *TESS* light curve data for the targets in this study. The observed SAP flux and corresponding Lomb–Scargle periodograms are presented in the subsequent figures. Although these recent *TESS* observations have noticeably lower photometric precision than the archival

Kepler/K2 data, we successfully recovered the main pulsation frequencies for HD 155291, HD 159571, and HD 138872 (Figure A2, A3, and A4). In contrast, the TESS data for HD 315823 (Figure A5) are noise-dominated, exhibiting no coherent signals across the three observed sectors.

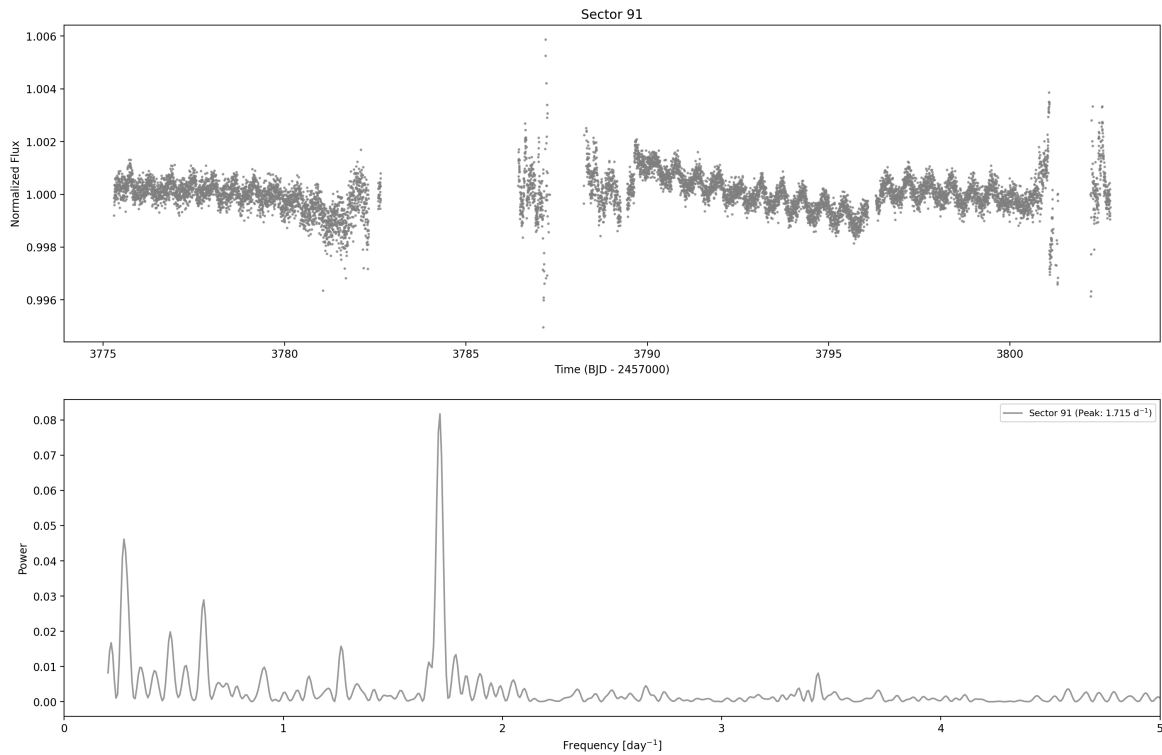


**Figure A2.** TESS light curve (top) and Lomb–Scargle periodogram (bottom) for HD 155291 (TIC 101669617).

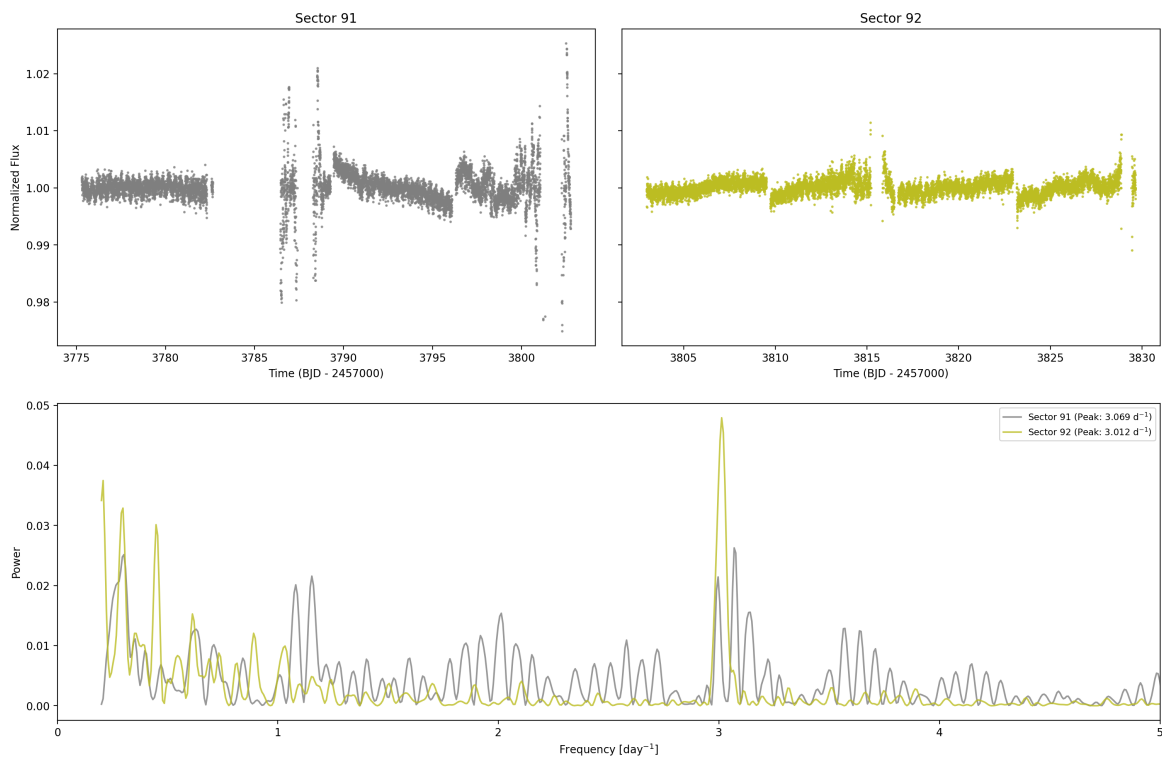


**Figure A3.** TESS light curves (top) and Lomb–Scargle periodograms (bottom) for HD 159571 (TIC 199983403), sectors 91 and 92.

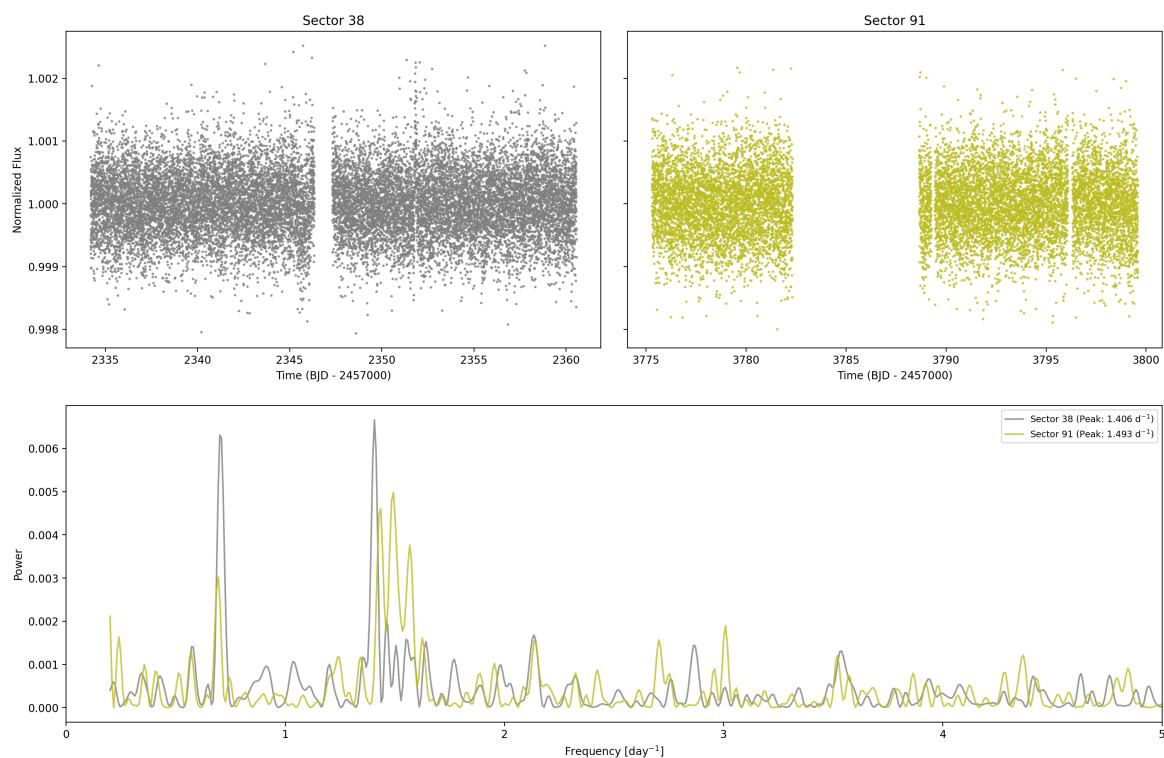


**Figure A4.** TESS light curves (top) and Lomb–Scargle periodograms (bottom) for HD 138872 (TIC 186902398), sectors 38 and 91.

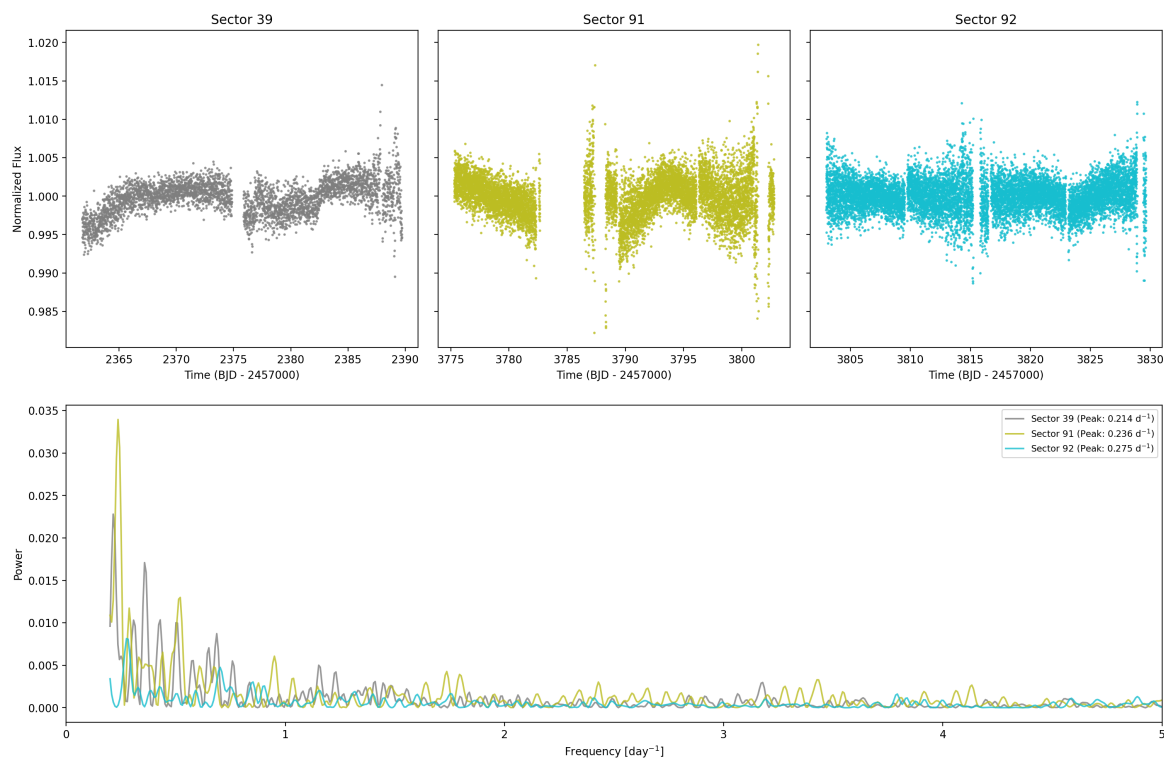


**Figure A5.** TESS light curves (top) and Lomb–Scargle periodograms (bottom) for HD 315823 (TIC 187134762), sectors 39, 91 and 92.

## References

1. Rivinius, T.; Carciofi, A.C.; Martayan, C. Classical Be stars. Rapidly rotating B stars with viscous Keplerian decretion disks. *Astron. Astrophys. Rev.* **2013**, *21*, 69, [arXiv:astro-ph.SR/1310.3962]. <https://doi.org/10.1007/s00159-013-0069-0>.

2. Auvergne, M.; Bodin, P.; Boissard, L.; Buey, J.T.; Chaintreuil, S.; Epstein, G.; Jouret, M.; Lam-Trong, T.; Levacher, P.; Magnan, A.; et al. The CoRoT satellite in flight: Description and performance. *Astron. Astrophys.* **2009**, *506*, 411–424, [arXiv:astro-ph.SR/0901.2206]. <https://doi.org/10.1051/0004-6361/200810860>.
3. Caldwell, D.A.; Cleve, J.E.V.; Jenkins, J.M.; Argabright, V.S.; Kolodziejczak, J.J.; Dunham, E.W.; Geary, J.C.; Tenenbaum, P.; Chandrasekaran, H.; Li, J.; et al. Kepler instrument performance: An in-flight update. In Proceedings of the Space Telescopes and Instrumentation 2010: Optical, Infrared, and Millimeter Wave; Jr., J.M.O.; Clampin, M.C.; MacEwen, H.A., Eds. International Society for Optics and Photonics, SPIE, 2010, Vol. 7731, p. 773117. <https://doi.org/10.1117/12.856638>.
4. Ricker, G.R.; Latham, D.W.; Vanderspek, R.K.; Ennico, K.A.; Bakos, G.; Brown, T.M.; Burgasser, A.J.; Charbonneau, D.; Deming, L.D.; Doty, J.P.; et al. The Transiting Exoplanet Survey Satellite (TESS). In Proceedings of the American Astronomical Society Meeting Abstracts #213, 2009, Vol. 213, *American Astronomical Society Meeting Abstracts*, p. 403.01.
5. Pereira, A.W.; Janot-Pacheco, E.; Andrade, L.; Emilio, M. The persistent Be enigma: The case of HD 212044. *Astron. Astrophys.* **2024**, *691*, L4. <https://doi.org/10.1051/0004-6361/202452215>.
6. Andrade, L.; Pereira, A.W.; Emilio, M.; Janot-Pacheco, E. Exploring the Variability of Three Be Stars with TESS Observations. *Universe* **2025**, *11*, 71. <https://doi.org/10.3390/universe11020071>.
7. Pereira, A.W.; Janot-Pacheco, E.; Emilio, M.; Andrade, L.; Armstrong, J.D.; Eidam, J.M.; Rabello-Soares, M.C.; da Silva, B.V.H.V. Characterizing B stars from Kepler/K2 Campaign 11. Optical analysis and seismic diagnostics. *Astron. Astrophys.* **2024**, *686*, A20. <https://doi.org/10.1051/0004-6361/202346439>.
8. Silva, B.V.H.V.d.; Eidam, J.M.; Pereira, A.W.; Rabello-Soares, M.C.; Janot-Pacheco, E.; Andrade, L.; Emilio, M. A Catalog of 73 B-Type Stars and Their Brightness Variation from K2 Campaign 13–18. *Universe* **2025**, *11*, 301. <https://doi.org/10.3390/universe11090301>.
9. Aigrain, S.; Parviainen, H.; Pope, B.J.S. K2SC: Flexible systematics correction and detrending of K2 light curves using Gaussian process regression. *Mon. Not. R. Astron. Soc.* **2016**, *459*, 2408–2419, [arXiv:astro-ph.SR/1603.09167]. <https://doi.org/10.1093/mnras/stw706>.
10. Vanderburg, A.; Johnson, J. A Technique for Extracting Highly Precise Photometry for the Two-Wheeled Kepler Mission. *Publications of the Astronomical Society of the Pacific* **2014**, *126*, 948–958. <https://doi.org/10.1086/678764>.
11. Scargle, J.D. Studies in astronomical time series analysis. II - Statistical aspects of spectral analysis of unevenly spaced data. *Astrophys. J.* **1982**, *263*, 835–853. <https://doi.org/10.1086/160554>.
12. Degroote, P.; Aerts, C.; Ollivier, M.; Miglio, A.; Debosscher, J.; Cuypers, J.; Briquet, M.; Montalbán, J.; Thoul, A.; Noels, A.; et al. CoRoT's view of newly discovered B-star pulsators: Results for 358 candidate B pulsators from the initial run's exoplanet field data. *Astron. Astrophys.* **2009**, *506*, 471–489, [arXiv:astro-ph.SR/0907.2183]. <https://doi.org/10.1051/0004-6361/200911884>.
13. Baran, A.S.; Koen, C.; Pokrzywka, B. A detection threshold in the amplitude spectra calculated from Kepler data obtained during K2 mission. *Monthly Notices of the Royal Astronomical Society: Letters* **2014**, *448*, L16–L19. <https://doi.org/10.1093/mnrasl/slu194>.
14. Tody, D. The IRAF Data Reduction and Analysis System. In Proceedings of the Instrumentation in astronomy VI; Crawford, D.L., Ed., 1986, Vol. 627, *Society of Photo-Optical Instrumentation Engineers (SPIE) Conference Series*, p. 733. <https://doi.org/10.1117/12.968154>.
15. Astropy Collaboration.; Robitaille, T.P.; Tollerud, E.J.; Greenfield, P.; Droettboom, M.; Bray, E.; Aldcroft, T.; Davis, M.; Ginsburg, A.; Price-Whelan, A.M.; et al. Astropy: A community Python package for astronomy. *Astron. Astrophys.* **2013**, *558*, A33, [arXiv:astro-ph.IM/1307.6212]. <https://doi.org/10.1051/0004-6361/201322068>.
16. Astropy Collaboration.; Price-Whelan, A.M.; Lim, P.L.; Earl, N.; Starkman, N.; Bradley, L.; Shupe, D.L.; Patil, A.A.; Corrales, L.; Brasseur, C.E.; et al. The Astropy Project: Sustaining and Growing a Community-oriented Open-source Project and the Latest Major Release (v5.0) of the Core Package. *Astrophys. J.* **2022**, *935*, 167, [arXiv:astro-ph.IM/2206.14220]. <https://doi.org/10.3847/1538-4357/ac7c74>.
17. Houk, N. *Michigan Catalogue of Two-dimensional Spectral Types for the HD stars. Volume\_3. Declinations -40\_f0 to -26\_f0*; 1982.
18. Morgan, W.W.; Abt, H.A.; Tapscott, J.W. *Revised MK Spectral Atlas for stars earlier than the sun*; 1978.
19. Gray, R.O.; Corbally, J., C. *Stellar Spectral Classification*; 2009.
20. Giridhar, S. Advances in spectral classification. *Bulletin of the Astronomical Society of India* **2010**, *1*, 1–33, [arXiv:astro-ph.SR/1004.1294]. <https://doi.org/10.48550/arXiv.1004.1294>.
21. Bowman, D.M.; Burssens, S.; Pedersen, M.G.; Johnston, C.; Aerts, C.; Buysschaert, B.; Michielsen, M.; Tkachenko, A.; Rogers, T.M.; Edelmann, P.V.F.; et al. Low-frequency gravity waves in blue super-

- giants revealed by high-precision space photometry. *Nature Astronomy* **2019**, *3*, 760–765, [arXiv:astro-ph.SR/1905.02120]. <https://doi.org/10.1038/s41550-019-0768-1>.
22. Bowman, D.M.; Aerts, C.; Johnston, C.; Pedersen, M.G.; Rogers, T.M.; Edelmann, P.V.F.; Simón-Díaz, S.; Van Reeth, T.; Buysschaert, B.; Tkachenko, A.; et al. Photometric detection of internal gravity waves in upper main-sequence stars. I. Methodology and application to CoRoT targets. *Astron. Astrophys.* **2019**, *621*, A135, [arXiv:astro-ph.SR/1811.08023]. <https://doi.org/10.1051/0004-6361/201833662>.
  23. Bowman, D.M. Asteroseismology of high-mass stars: New insights of stellar interiors with space telescopes. *Frontiers in Astronomy and Space Sciences* **2020**, *7*, 70, [arXiv:astro-ph.SR/2008.11162]. <https://doi.org/10.3389/fspas.2020.578584>.
  24. Hirata, R. Disk Precession in Pleione. In Proceedings of the Active OB-Stars: Laboratories for Stellare and Circumstellar Physics; Okazaki, A.T.; Owocki, S.P.; Stefl, S., Eds., 2007, Vol. 361, *Astronomical Society of the Pacific Conference Series*, p. 267.
  25. Nemravová, J.; Harmanec, P.; Kubát, J.; Koubský, P.; Iliev, L.; Yang, S.; Ribeiro, J.; Šlechta, M.; Kotková, L.; Wolf, M.; et al. Properties and nature of Be stars. 27. Orbital and recent long-term variations of the Pleiades Be star Pleione = BU Tauri. *Astron. Astrophys.* **2010**, *516*, A80, [arXiv:astro-ph.SR/1003.5625]. <https://doi.org/10.1051/0004-6361/200913885>.
  26. Houk, N.; Smith-Moore, M. *Michigan Catalogue of Two-dimensional Spectral Types for the HD Stars. Volume 4, Declinations -26°.0 to -12°.0.*; Vol. 4, 1988.
  27. Wallenquist, Å. A study of the distribution of the stars in the Sagittarius and Ophiuchius regions of the Milky Way. *Annals of the Bosscha Observatory Lembang (Java) Indonesia* **1939**, *5*, E1–E138.
  28. McSwain, M.V.; Huang, W.; Gies, D.R. Variability of Be Stars in Southern Open Clusters. *Astrophys. J.* **2009**, *700*, 1216–1232, [arXiv:astro-ph.SR/0905.0640]. <https://doi.org/10.1088/0004-637X/700/2/1216>.
  29. Bernhard, K.; Otero, S.; Hümmerich, S.; Kaltcheva, N.; Paunzen, E.; Bohlsen, T. An investigation of the photometric variability of confirmed and candidate Galactic Be stars using ASAS-3 data. *Mon. Not. R. Astron. Soc.* **2018**, *479*, 2909–2967, [arXiv:astro-ph.SR/1805.07665]. <https://doi.org/10.1093/mnras/sty1320>.
  30. Burssens, S.; Simón-Díaz, S.; Bowman, D.M.; Holgado, G.; Michielsen, M.; de Burgos, A.; Castro, N.; Barbá, R.H.; Aerts, C. Variability of OB stars from TESS southern Sectors 1-13 and high-resolution IACOB and OWN spectroscopy. *Astron. Astrophys.* **2020**, *639*, A81, [arXiv:astro-ph.SR/2005.09658]. <https://doi.org/10.1051/0004-6361/202037700>.
  31. Jian, M.; Matsunaga, N.; Jiang, B.; Yuan, H.; Zhang, R. Exploring Be phenomena in OBA stars: A mid-infrared search. *Astron. Astrophys.* **2024**, *682*, A59, [arXiv:astro-ph.SR/2311.08395]. <https://doi.org/10.1051/0004-6361/202347911>.
  32. Figueiredo, A.L.; Carciofi, A.C.; Labadie-Bartz, J.; Pinho, M.L.; de Amorim, T.H.; Ticiani dos Santos, P.; Soszyński, I.; Udalski, A. Be Star Demographics: A Comprehensive Study of Thousands of Light Curves in the Magellanic Clouds. *Astrophys. J.* **2025**, *994*, 58, [arXiv:astro-ph.SR/2505.08714]. <https://doi.org/10.3847/1538-4357/ae0612>.
  33. Rauer, H.; Aerts, C.; Cabrera, J.; Deleuil, M.; Erikson, A.; Gizon, L.; Goupil, M.; Heras, A.; Walloschek, T.; Lorenzo-Alvarez, J.; et al. The PLATO mission. *Experimental Astronomy* **2025**, *59*, 26, [arXiv:astro-ph.IM/2406.05447]. <https://doi.org/10.1007/s10686-025-09985-9>.

**Disclaimer/Publisher's Note:** The statements, opinions and data contained in all publications are solely those of the individual author(s) and contributor(s) and not of MDPI and/or the editor(s). MDPI and/or the editor(s) disclaim responsibility for any injury to people or property resulting from any ideas, methods, instructions or products referred to in the content.